Behavioral/Cognitive

Structural Variability within Frontoparietal Networks and Individual Differences in Attentional Functions: An Approach Using the Theory of Visual Attention

Magdalena Chechlacz,[1] Celine R. Gillebert,[1] Signe A. Vangkilde,[2] Anders Petersen,[2] and Glyn W. Humphreys[1]
[1]Department of Experimental Psychology, University of Oxford, Oxford OX1 3UD, United Kingdom, and [2]Department of Psychology, Center for Visual Cognition, University of Copenhagen, 1353 Copenhagen, Denmark

Visuospatial attention allows us to select and act upon a subset of behaviorally relevant visual stimuli while ignoring distraction. Bundesen's theory of visual attention (TVA) (Bundesen, 1990) offers a quantitative analysis of the different facets of attention within a unitary model and provides a powerful analytic framework for understanding individual differences in attentional functions. Visuospatial attention is contingent upon large networks, distributed across both hemispheres, consisting of several cortical areas interconnected by long-association frontoparietal pathways, including three branches of the superior longitudinal fasciculus (SLF I-III) and the inferior fronto-occipital fasciculus (IFOF). Here we examine whether structural variability within human frontoparietal networks mediates differences in attention abilities as assessed by the TVA. Structural measures were based on spherical deconvolution and tractography-derived indices of tract volume and hindrance-modulated orientational anisotropy (HMOA). Individual differences in visual short-term memory (VSTM) were linked to variability in the microstructure (HMOA) of SLF II, SLF III, and IFOF within the right hemisphere. Moreover, VSTM and speed of information processing were linked to hemispheric lateralization within the IFOF. Differences in spatial bias were mediated by both variability in microstructure and volume of the right SLF II. Our data indicate that the microstructural and macrostrucutral organization of white matter pathways differentially contributes to both the anatomical lateralization of frontoparietal attentional networks and to individual differences in attentional functions. We conclude that individual differences in VSTM capacity, processing speed, and spatial bias, as assessed by TVA, link to variability in structural organization within frontoparietal pathways.

Key words: **diffusion tractography; frontoparietal attention networks; individual differences; theory of visual attention; visuospatial memory**

Introduction

Within the visual scene, multiple stimuli compete for neural representation and the allocation of processing resources. The cognitive abilities collectively defined as "visual attention" allow us to select and act upon a subset of behaviorally relevant visual stimuli while ignoring the rest. Over the past 30 years, various models have been proposed to account for the varied aspects of visual attention and to model attentional limits on information processing (Neisser, 1967; Treisman and Gelade, 1980). Among these, Bundesen's theory of visual attention (TVA) is one of the few that offers a quantitative analysis of the different facets of attention within a unitary framework (Bundesen, 1990; Bundesen et al., 2005). TVA is closely related to the idea that attentional selection operates through biasing the competition between stimuli for the control of action (Desimone and Duncan, 1995; Duncan et al., 1997). Behavioral performance on numerous daily living tasks varies depending on differences in attentional abilities. Although individual differences in human cognition and behavior are widely reported and linked to variability in brain structure and function (Rademacher et al., 2001; Boorman et al., 2007; Sugiura et al., 2007; Roberts et al., 2010; Frost and Goebel, 2012; Mueller et al., 2013), how individual differences in attentional abilities map to variability in brain architecture is poorly understood.

Functional and structural neuroimaging studies show that visual attention is contingent upon large and distributed neuronal networks consisting of several cortical areas subdivided into functionally distinct dorsal and ventral components (Mesulam, 1990; Corbetta and Shulman, 2002; Szczepanski et al., 2013) interconnected by long-association frontoparietal pathways, including the superior longitudinal fasciculus (SLF) and the inferior fronto-occipital fasciculus (IFOF) (Bartolomeo et al.,

Received Jan. 15, 2015; revised May 11, 2015; accepted May 13, 2015.

Author contributions: M.C. and G.W.H. designed research; M.C. performed research; S.A.V. and A.P. contributed unpublished reagents/analytic tools; M.C. and C.R.G. analyzed data; M.C., C.R.G., and G.W.H. wrote the paper.

This work was supported by the National Institute of Health Research (Oxford Cognitive Health Clinical Research Facility) to G.W.H., M.C. holds a British Academy Postdoctoral Fellowship. C.R.G. holds a Sir Henry Wellcome Postdoctoral Fellowship funded by Wellcome Trust Grant 098771/Z/12/Z. We thank Dr. Stamatios Sotiropoulos (FMRIB Analysis Group) for help with preprocessing and distortion correction of diffusion-weighted MRI data.

The authors declare no competing financial interests.

This article is freely available online through the *J Neurosci* Author Open Choice option.

Correspondence should be addressed to Dr. Magdalena Chechlacz, Department of Experimental Psychology, Oxford University, 9 South Parks Road, Oxford OX1 3UD, UK. E-mail: magdalena.chechlacz@psy.ox.ac.uk.

DOI:10.1523/JNEUROSCI.0210-15.2015

2007; Schmahmann et al., 2007; Doricchi et al., 2008; Thiebaut de Schotten et al., 2011). A recent study used diffusion imaging and tractography to reconstruct three separate branches of the SLF (SLF I subserving the dorsal attention network, SLF II interconnecting the dorsal and ventral networks, and SLF III subserving the ventral attention network) and showed that variations in SLF II correlated with greater biases in both line bisection and in target detection (Thiebaut de Schotten et al., 2011). The data indicate that individual differences in attention may be causally linked to variability within neural networks, specifically that lateralization within white matter (WM) pathways predicts attentional bias in behavioral performance. A recent fMRI study also demonstrated a strong relationship between (1) variability in a neural index of spatial bias (measured as the relative strengths of attentional responses within frontoparietal areas within the right hemisphere, which were calculated based on an fMRI covert attention task) and (2) individual differences in spatial bias in behavior (calculated based on performance in a landmark task) (Szczepanski and Kastner, 2013). However, given that line bisection and spatial bias in target detection only represent one facet of the full spectrum of attentional abilities and underlying cognitive mechanisms, any conclusions relating to individual differences in attentional function remain tentative.

Here we conducted detailed analysis to assess whether structural variability within frontoparietal networks (SLF I, SLF II, SLF III, and IFOF) mediates differences in multiple visual attention parameters derived from the TVA: processing speed, visual short-term memory capacity, spatial bias, the minimum effective exposure duration, and the top-down controlled selection. Measures of macrostructural and microstructural variability within frontoparietal networks were based on recent methodological advances in diffusion imaging, spherical deconvolution and tractography-derived indices of tract volume, and hindrance-modulated orientational anisotropy (Dell'Acqua et al., 2013).

Materials and Methods

Participants. A total of 48 healthy volunteers participated. We excluded participants with a previous history of neurological or psychiatric disorders and contraindications to MRI based on a semistructured interview. All participants provided written informed consent in accordance with protocols approved by the Oxford Research Ethics Committee. Image artifacts were identified on one of the MRI datasets; consequently, this participant was excluded from the study. Data from 47 participants were entered into the analyses (18 males; mean ± SD age, 26.9 ± 5.1 years).

Left-handed participants are regularly excluded from neuroscience studies, mainly to reduce variance in the data. Although it has been suggested that some left-handed participants have atypically lateralized brain functions, the link between handedness and brain lateralization is not straightforward (Bryden et al., 1983; Sommer et al., 2002; Szaflarski et al., 2002; Flöel et al., 2005; Whitehouse and Bishop, 2009; Badzakova-Trajkov et al., 2010; Cai et al., 2013; Mazoyer et al., 2014; for a recent comprehensive review, see Willems et al., 2014). As our study focused on individual differences, we did not select our participants based on handedness to better represent normal variation in the human population (with ~10% of left-handed individuals) (Willems et al., 2014). We used the Edinburgh Handedness Inventory (Oldfield, 1971) to assess handedness in the studied group. The scale ranges from −100 (extremely left-handed; score below −40 left-handedness) to 100 (extremely right-handed; score above 40 right-handedness) and the score between −40 to 40 indicate ambidexterity. The full score based on the Edinburgh Handedness Inventory was entered into the analyses. Full demographic data, including handedness, are presented in Table 1.

Behavioral testing. TVA parameters are derived using established procedures with briefly presented, multi-item displays under conditions when participants are asked to identify all the items (whole report, where memory capacity can be measured) or/and when participants are cued to report only a subset of stimuli with certain features (partial report, to measure attentional selection) (Bundesen, 1990). Previous studies using experimental procedures equivalent to those used in the current study (as described below) have shown good internal reliability and accuracy of TVA measures based on bootstrap statistics enabling experimenters to calculate the measurement error related to each attention parameter estimated within a single testing session (Habekost and Bundesen, 2003; Finke et al., 2005; Habekost and Rostrup, 2006). Earlier work has also provided strong evidence of the test–retest reliability of TVA-based measures (Habekost et al., 2014). In the current study, we used the "CombiTVA" paradigm designed as a combination of the two classical experimental approaches, whole report and partial report, allowing full assessment of distinct facets of visual attention within a single task (Vangkilde et al., 2011).

Table 1. Participants' demographic data

Participant	Age (yr)	Gender	Handedness[a]	Participant	Age (yr)	Gender	Handedness[a]
P01	32	F	100	P25	28	F	73
P02	21	F	100	P26	28	M	88
P03	20	M	87	P27	32	F	−20
P04	33	F	−71	P28	20	F	90
P05	36	M	100	P29	22	M	−100
P06	26	F	100	P30	24	F	82
P07	25	M	20	P31	28	F	100
P08	28	F	70	P32	24	M	37
P09	32	F	0	P33	29	M	81
P10	33	F	73	P34	26	M	53
P11	34	M	30	P35	22	M	−30
P12	36	M	100	P36	23	F	100
P13	30	F	100	P37	21	M	100
P14	24	F	0	P38	33	F	88
P15	24	F	85	P39	22	F	100
P16	32	F	90	P40	21	F	−33
P17	32	F	−78	P41	28	F	90
P18	27	F	−100	P42	32	M	88
P19	20	M	100	P43	24	M	46
P20	28	M	90	P44	22	M	−30
P21	20	F	−73	P45	24	F	100
P22	36	F	−67	P46	36	F	50
P23	21	F	76	P47	21	M	0
P24	24	F	73				

[a]Edinburgh Handedness Inventory (Oldfield, 1971).

F, female; M, male.

At the beginning of the testing session, all participants were seated in a semidark room ~60 cm from the ViewSonic 23 inch LED monitor (set at 100 Hz frequency). The CombiTVA paradigm (Vangkilde et al., 2011) was presented using E-prime 2 Professional software (Psychology Software Tools). The entire CombiTVA paradigm took 45 min to complete and was divided into nine experimental blocks, each consisting of 36 trials, which followed 24 practice trials. All trials shared the same basic design as illustrated in Figure 1. The initial screen, with a red fixation cross presented in the middle of a black field, was followed by a 100 ms blank screen, followed by a variable letter stimulus display (see below) presented around an imaginary circle ($r = 7.5°$ of visual angle) with six possible stimulus locations. The stimulus display was followed by a mask presented for 500 ms (made from red and blue letter fragments completely covering the six stimulus locations) and finally by a black screen indicating that the participants should respond by typing in the letters that they had seen. The response time was unlimited. The whole report trials used red target letters with either two items presented for 80 ms or six items presented for one of six stimulus durations: 10, 20, 50, 80, 140, or 200 ms. The partial report trials consisted of two red target letters and four blue distractor letters presented for 80 ms. All trials were intermixed and featured as stimuli different letters randomly chosen from a set of 20 capital letters (ABDEFGHJKLMNOPRSTVXZ) with font size corresponding to 2.7° × 2.3° of visual angle.

Before testing, all participants were told that the speed of their response was irrelevant and they should report all the red letters they were

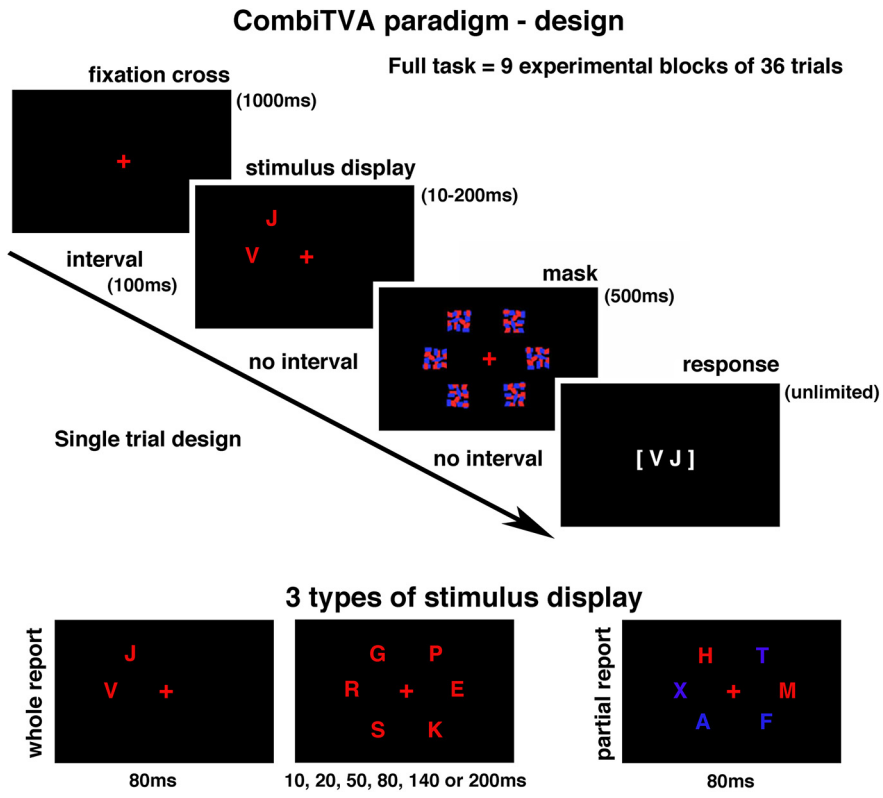

Figure 1. CombiTVA paradigm: stimulus display conditions (whole report and partial report) and experimental design.

"fairly certain" of having seen and to refrain from pure guessing. Participants were told that the accuracy of their reports (based only on reported but not missed letters) would be given after each block. Although we encouraged participants to report as many red letters as possible, we also asked then to keep their reports within an accuracy range of 80%–90% correct. As the behavioral output from each participant, we recorded the number of correctly reported target letters on each trial, and this output was entered into the analysis as the main dependent variable.

Estimation of TVA parameters. We used a previously developed maximum likelihood fitting procedure to model performance of all participants based on the TVA framework (for full details, see Kyllingsbaek, 2006; Dyrholm et al., 2011). Briefly, the maximum likelihood fitting procedure assessed attentional abilities in terms of five parameters: (1) visual short-term memory (VSTM) capacity measured by the number of reported letters (parameter K; K was assumed to vary on a trial-by-trial basis); (2) the speed of visual information processing (parameter C), measured in terms of the number of letters processed per second; (3) the minimum exposure duration for conscious perception (parameter t_0), defined as the longest ineffective exposure duration of the letter display and measured in seconds; (4) top-down controlled selection (attentional weight of distractors as opposed to targets; parameter α), calculated as the ratio between the attentional weight of distractors and the attentional weight of targets; α values close to 0 indicate efficient selection of targets over distractors, values close to 1 indicate no prioritizing of targets compared with distracters, and values >1 indicate that distractors were selected more than targets; in this definition, top-down controlled selection is based on nonspatial properties of the stimuli (e.g., their color) and so should be distinguished from top-down spatial selection; and (5) the laterality index (ω_{index}), indicating differential attentional weighting between elements in the left versus the right visual field (i.e., a measure of spatial bias calculated from the ratio between the sum of attentional weights assigned to elements in the left hemifield and the sum of attentional weights across the entire visual field; a value of 0.5 indicates unbiased spatial weighting of attention, values <0.5 indicate a rightward bias, and values >0.5 indicate a leftward bias). Figure 2 illustrates the relationship between the raw data and the five parameters calculated using the methods described above.

We also applied a more complex model with different attentional weights for each of the six letter locations; as parameter estimates were very similar across both models, the first model with the fewest degrees of freedom was preferred.

MRI data acquisition. Diffusion-weighted scans were acquired at the Oxford Centre for Functional Magnetic Resonance Imaging of the Brain (FMRIB) using a 3T Verio scanner with a 32-channel head coil (Siemens). Diffusion-weighted data were acquired using EPI and a generalized autocalibrating partially parallel acquisition sequence with a voxel size of $2 \times 2 \times 2$ mm^3 and the following parameters: TR = 9600 ms and TE = 87 ms. The diffusion weighting was isotropically distributed along the 60 directions (b = 1500 s/mm^2) plus 4 volumes were acquired without diffusion weighting. To improve the signal-to-noise ratio and to minimize geometric distortion resulting from EPI acquisition, for each participant two sets of whole-brain diffusion-weighted data were acquired with the dual-echo blip-reversed sequence. As a result, the two sets of images had phase-encoded direction reversed ("blip-up" and "blip-down") and thus had geometric distortions of equal magnitude but going in the opposite direction, enabling us to calculate a corrected image (Chang and Fitzpatrick, 1992; Andersson et al., 2003). Diffusion-weighted images were preprocessed for distortion correction as in Sotiropoulos et al. (2013) using the latest FSL tools (FMRIB Centre Software Library, Oxford University) (Smith et al., 2004). Briefly, pairs of phase-reversed images were used to correct for susceptibility-induced distortions (Andersson et al., 2003) using the FSL TOPUP tool. Eddy currents and subject motion were corrected using a generative model approach (Sotiropoulos et al., 2013) using the FSL EDDY tool.

Spherical deconvolution and tractography. Frontoparietal pathways are located within a complex WM architecture, with high WM density and multiple crossing fibers from numerous neuronal pathways (Thiebaut de Schotten et al., 2011). Therefore, we used a spherical deconvolution approach based on modeling the diffusion signal as a distribution of multiple fiber orientations as it allows quantification of WM properties in the regions of crossing fibers and thus overcomes some of the limitations of more traditional tractography methods (Dell'Acqua et al., 2013). We applied a spherical deconvolution approach based on the damped Richardson-Lucy algorithm as implemented in the StarTrack software (www.natbrainlab.com) with algorithm parameters chosen as previously described (Dell'Acqua et al., 2010, 2013). Subsequently, we performed whole-brain tractography with the StarTrack software with streamlines propagated using an Euler integration with a step size of 0.5 mm and an angular threshold of 45°. Finally, we performed virtual dissections of frontoparietal pathways (SLF I, SLF II, SLF III, and IFOF) using TrackVis (Ruopeng Wang, Van J. Wedeen, TrackVis.org, Martinos Center for Biomedical Imaging, Massachusetts General Hospital). For the three branches of the superior longitudinal fasciculus (SLF I, SLF II, SLF III), a multiple ROIs approach was used as previously described (Thiebaut de Schotten et al., 2011). Four ('AND') ROIs were defined around the superior, middle and inferior frontal gyri and posteriorly in the parietal region within both hemispheres. A final ('NOT') ROI was defined in temporal lobe of each hemisphere to exclude fibers of the arcuate fasciculus (Fig. 3*A*). A two-ROI approach was used for the IFOF (Mori et al., 2002; Catani and Thiebaut de Schotten, 2008). As the IFOF connects the frontal and occipital lobes, within both the left and the right hemisphere,

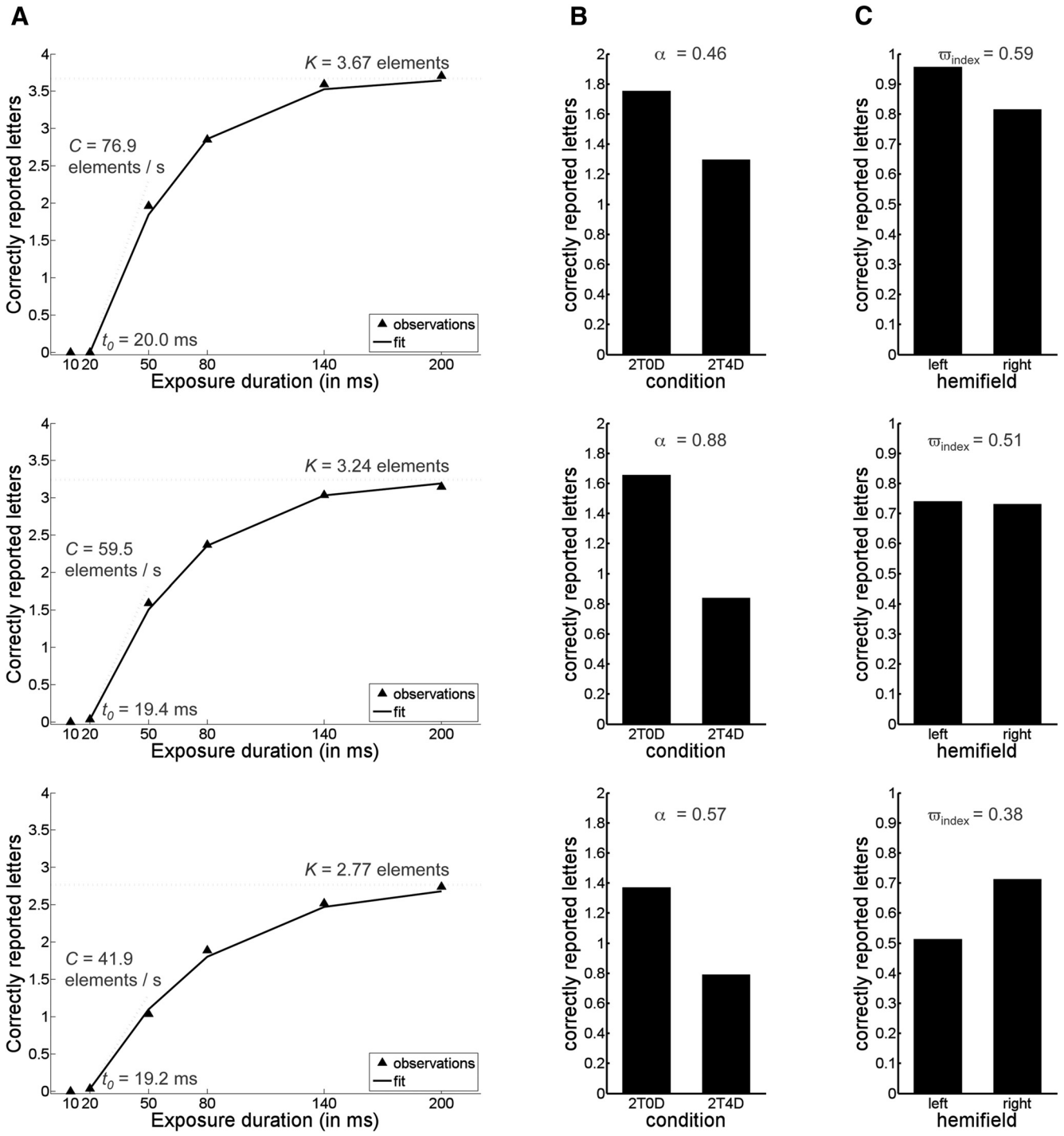

Figure 2. The raw data plots from three representative participants illustrating the relationship between the raw data and the five calculated parameters. ***A***, Whole report data when 6 targets are presented at the different exposure duration. In addition to the plotted raw scores/observations (black triangles), the scores predicted by the TVA model are plotted (solid black line) to indicate that the model is a good fit to the data and to illustrate how K, C, and t_0 parameters are related to these scores. ***B***, The data when 2 targets are presented with and without distractors (2T4D = 2 targets and 4 distractors; 2T0D = 2 targets and 0 distractors). The difference between both conditions relates to α parameter. ***C***, Average number of correctly reported letters in the left and right visual field (averaged across all conditions in the experiment). The difference between both conditions measures the laterality index (ω_{index}). To further assess the relationship between raw data and the calculated TVA parameters, we performed correlation analyses, which showed overall good correspondence between the raw and calculated measures. For example: (1) the raw scores for the whole report: 6 target letter condition (measuring the number of reported letters at the longest exposure duration, i.e., 200 ms) were strongly correlated with TVA-based K parameter ($r = 0.91$); (2) the difference in the raw scores between the number of correctly reported letters at 10 and 80 ms was strongly correlated with TVA-based parameter C ($r = 0.85$); (3) based on the raw scores for conditions 2T0D and 2T4D (2T4D = 2 targets and 4 distractors; 2T0D = 2 targets and 0 distractors), we calculated an attentional selection index 2T0D/(2T0D + 2T4D), which was strongly correlated with TVA-based α parameter ($r = 0.88$); and (4) based on the raw scores for the left and right visual fields, we calculated the following LI left/(left + right), which was strongly correlated with the TVA-based laterality index ($\omega_{index;}$ $r = 0.99$).

first ROI was defined within the frontal cortex and the second ROI was defined within the occipital cortex as illustrated in Figure 3*B*.

Following virtual dissection of the frontoparietal pathways, we extracted for each tract the hindrance-modulated orientational anisotropy (HMOA), an index characterizing WM diffusion properties and thus reflecting WM organization and microstructure (Dell'Acqua et al., 2013). We also calculated volume for each tract based on the number of voxels intersected by the streamlines of each tract as such measure de-

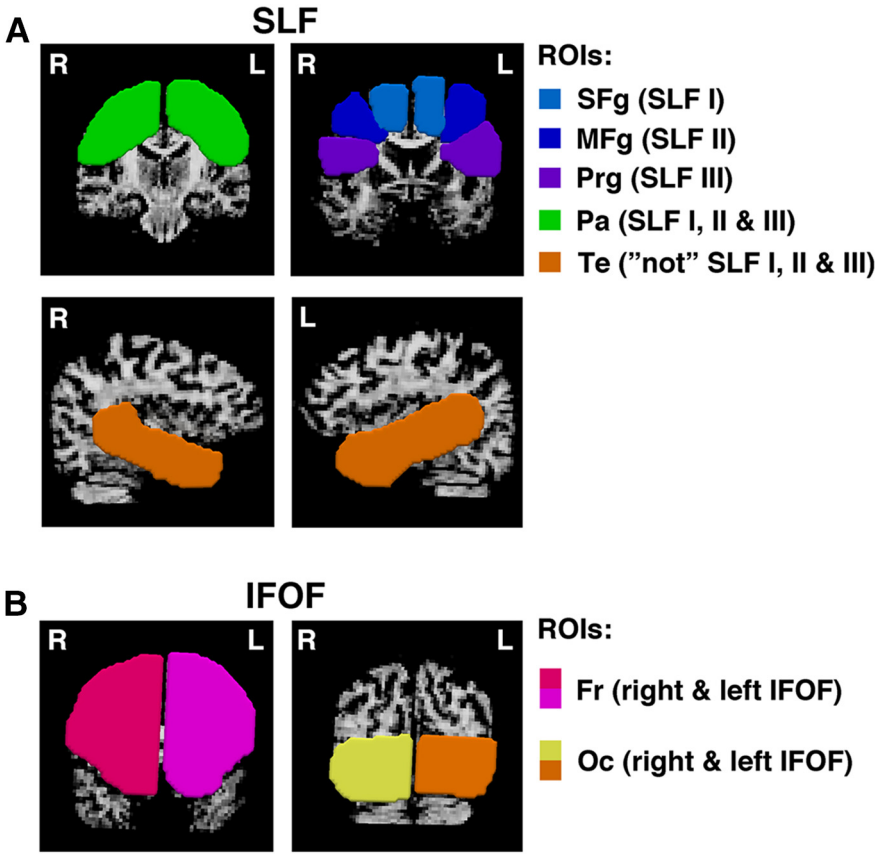

Figure 3. Location and delineation of ROIs used in spherical deconvolution tractography. ***A***, For the three branches of the SLF (I, II, and III), a multiple ROI approach was used (Thiebaut de Schotten et al., 2011). Frontal ROIs in the superior frontal gyrus (SFg), middle frontal gyrus (MFg), and precentral gyrus (Prg) were used for reconstruction of SLF I, SLF II, and SLF III, respectively, in the right and left hemisphere. These frontal ROIs were used in combination with a single parietal (Pa) ROI for all three branches of SLF in both hemispheres. A final "not" ROI was defined in temporal (Te) lobe of each hemisphere, to exclude fibers of the arcuate fasciculus. This "not" ROI was applied for the tractography of all three branches of SLF. ***B***, For the IFOF connecting the frontal and occipital lobes, we used two ROIs for both right and left hemispheres: one within frontal cortex (Fr) at the level where frontal and temporal lobes are separated and the other one within occipital cortex (Oc) at the level of parieto-occipital sulcus (Mori et al., 2002).

Table 2. Estimated TVA parameters and descriptive statistics

Parameter	Mean (SD) of estimated values	Correlation with age	Correlation with handedness
K	3.43 (0.62)	$r = -0.11; p = 0.47$	$r = 0.19; p = 0.21$
C	55.73 (18.68)	$r = 0.04; p = 0.79$	$r = 0.18; p = 0.22$
t_0	12.39 (7.67)	$r = 0.24; p = 0.10$	$r = 0.26; p = 0.09$
α	0.67 (0.31)	$r = 0.20; p = 0.99$	$r = 0.04; p = 0.79$
ω_{index}	0.48 (0.08)	$r = 0.13; p = 0.39$	$r = 0.01; p = 0.94$

notes the space occupied by the reconstructed pathway. As tractography was performed in the native space, to control for variability in brain/hemisphere size, which could affect the volume of the reconstructed tracts (larger brain = larger tract), for each participant we normalized the tract volume by the hemisphere WM volume (tract volume/hemisphere WM volume). The HMOA index and normalized tract volume were then used in the statistical analysis. In addition, we calculated the lateralization index (LI) for all the reconstructed frontoparietal pathways, with negative values indicating a leftward asymmetry and positive values indicating a rightward asymmetry, according to the following formula: LI = (right − left)/(right + left).

Statistical analyses. All statistical analyses were performed using MATLAB 7.14/R2012a (The MathWorks). We first used the Lilliefors test as implemented in MATLAB to verify the normal distribution of the data. The Gaussian distribution was confirmed for all variables, with the exception of parameter t_0. Next, Pearson correlation analyses were performed to examine the link between structural variability within the frontoparietal networks and individual differences in visual attention abilities as assessed by the TVA (processing speed, VSTM capacity, attentional weighting between left and right visual field/spatial bias, minimum effective exposure duration, top-down controlled selection). As the normal distribution was not confirmed for the parameter t_0, we have repeated correlation analyses between this variable and all macrostructural and microstructural measures for the frontoparietal pathways using Spearman's method. To correct for multiple comparisons in the analysis correlating the TVA-derived parameters with the measures of structural variability (HMOA, volume, LI), we applied FDR correction based on the Benjamini–Hochberg FDR method as implemented in MATLAB Bioinformatics toolbox (Benjamini and Hochberg, 1995). Unless specified otherwise, we report FDR corrected p values. One-sample t tests were used to access lateralization of the frontoparietal pathways. In addition, we also performed correlation analyses between the raw data from the CombiTVA task (Fig. 2) and microstructural and macrostructural measures of structural variability within the frontoparietal networks. The Lilliefors test, as implemented in MATLAB, was used to verify the normal distribution of the raw data.

Results

Behavioral data: attentional abilities

Using the mean number of correctly reported letters per condition, estimates of K, C, t_0, α, and ω_{index} were calculated using a maximum likelihood fitting procedure (Table 2). The estimates derived from our data are in agreement with those previously described for the corresponding age groups (see, e.g., Espeseth et al., 2014). Subsequently, we examined bivariate correlations between the different TVA-based parameters. We found a strong positive correlation between K, the VSTM capacity, and C, the speed of information processing ($r = 0.59$; $p < 0.00001$, uncorrected; this finding is in agreement with recent report by Habekost et al. (2014), and a weaker negative correlation between K and ω_{index}, corresponding to the attentional spatial bias ($r = -0.33$; $p < 0.02$, uncorrected). No other correlations were significant ($p > 0.05$).

Attentional abilities can be affected by age (Espeseth et al., 2014), but in the group of our relatively young participants (age range 20–36 years; Table 1), we found no correlation between any of the estimated TVA parameters and age (Table 2). In the current study, we have not excluded participants based on handedness; and according to the Edinburgh Handedness Inventory (Oldfield, 1971), 6 participants were classified as left-handed, 31 were classified as right-handed, and 10 were classified as ambidextrous. There were no correlations between the handedness measure and any of the TVA parameters in the examined group (Table 2). It should be noted, however, that the null correlations potentially resulted from a disproportionately large number of right-handed participants. Subsequently, we also compared the performance on the TVA task between the right-handed participants and either

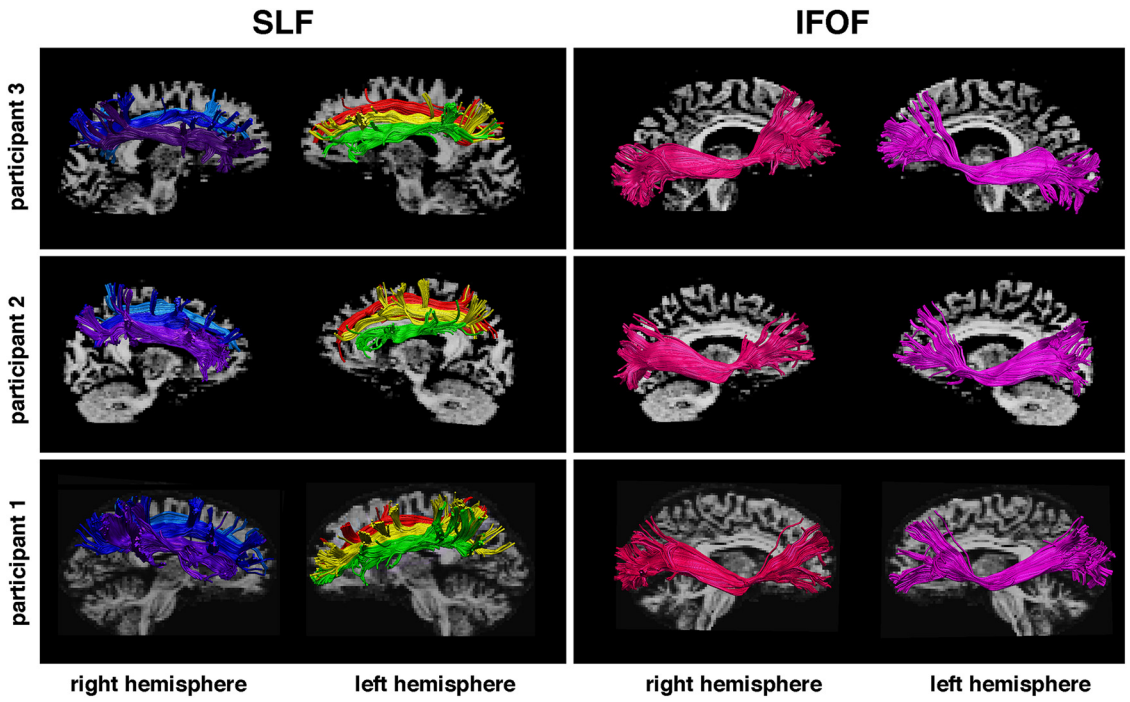

Figure 4. Examples of spherical deconvolution tractography reconstruction of the frontoparietal pathways in three participants. Three branches of the SLF, I (light blue and red), II (dark blue and yellow), and III (violet and green), and the IFOF (pink and purple) reconstructed within the right and the left hemispheres.

left-handed participants or all other participants (left-handers plus mixed-handers), and no significant differences were found ($p > 0.5$).

Neuroimaging data: structural variability as a predictor of attentional abilities

To assess structural variability of the frontoparietal connections within the attentional networks, we performed spherical deconvolution tractography of SLF I, SLF II, SLF III, and IFOF (Fig. 4) and then calculated HMOA index and volume for all four WM tracts in both hemispheres. These measures were used: (1) to examine structural lateralization within frontoparietal pathways and (2) to assess whether structural variability within the frontoparietal networks mediates individual differences in the TVA-derived parameters.

We first evaluated the lateralization of frontoparietal pathways based on HMOA and found that, based on this microstructural index, the SLF I and SLF III were symmetrically organized (all p values > 0.1), whereas SLF II and IFOF were right lateralized (SLF II $t_{(46)} = 4.62$, $p < 0.000031$; IFOF $t_{(46)} = 2.81$, $p = 0.0071$), although the observed hemispheric lateralization of IFOF was relatively weaker (Fig. 5). We next compared a macrostructural laterality index based on tract volumes. Using this index, we found that SLF III was strongly right lateralized ($t_{(46)} = 6.96$, $p = 1.04 \times 10^{-8}$), whereas SLF II and IFOF were symmetrically distributed between left and right hemispheres (SLF II $t_{(46)} = -0.32$, $p = 0.75$; IFOF $t_{(46)} = 1.32$, $p = 0.19$). Finally, we found a weak trend for left lateralization of SLF I ($t_{(46)} = -2.57$, $p = 0.034$). Our data indicate differential hemispheric organization of fiber tracts depending upon whether microstructural or macrostructural indices are taken.

In the studied group, 6 participants were classified as left-handed and 10 were classified as ambidextrous, which potentially makes the lateralization results harder to interpret. Therefore, we reexamined lateralization of frontoparietal pathways while including only right-handed participants. These repeated analyses yielded alike results. Based on HMOA index, we found the SLF II and IFOF to be right lateralized (SLF II $t_{(30)} = 4.95$, $p < 0.000026$; IFOF $t_{(30)} = 2.28$, $p = 0.03$) and the SLF I and SLF III to be symmetrically organized ($p > 0.1$). Subsequently, using laterality index calculated based on tract volume, we found SLF III to be right lateralized ($t_{(30)} = 5.27$, $p < 0.00001$), whereas other pathways were symmetrically organized ($p > 0.1$).

Interestingly, we found no correlations between the lateralization indices (calculated based on either tract volume or HMOA index) of any the reconstructed frontoparietal pathways and either the handedness measure or age in the examined group of participants (all p values not significant, i.e., $p > 0.1$). It should be noted, however, that the null correlations with handedness potentially resulted from a disproportionately large number of right-handed participants. As our aim was to study individual differences in visual attention and structural variability, we have not preselected our participants to represent normal variation in the human population (~10% of left-handed individuals) (Willems et al., 2014). A recent study (Petit et al., 2015) provides interesting evidence on the link between functional right hemisphere dominance and handedness. Petit et al. (2015) showed that, in a large group of 293 preselected participants (98 strongly left-handed, 98 with mixed-handedness and 97 strongly right-handed), functional right hemispheric dominance within the ventral network occurred regardless of both hand preference and eye preference. They also found that, regardless of eye preference, left-handed participants showed a strong rightward asymmetry in the dorsal network. This is particularly relevant as it has been suggested by some, but contradicted by others, that left-handers show left-hemisphere dominance for attention and right language lateralization (Bryden et al., 1983; Flöel et al., 2005; Whitehouse and Bishop, 2009; Badzakova-Trajkov et al., 2010; Cai et al., 2013). Although, in the current study we had a large number of right-handed participants compared with left- and mixed-

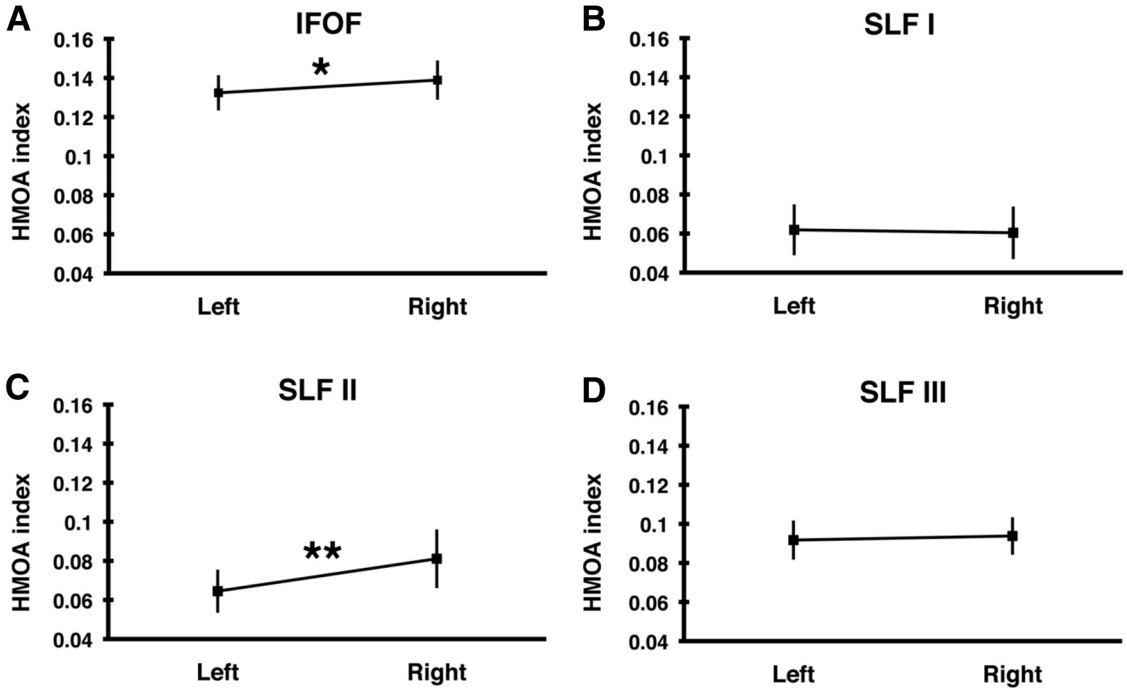

Figure 5. Hemispheric lateralization of the frontoparietal pathways. Mean HMOA index (±SD) of (***A***) the IFOF and the three branches of superior longitudinal fasciculus: (***B***) SLF I, (***C***) SLF II, and (***D***) SLF III in the left and right hemispheres. *$p < 0.01$. **$p < 0.00005$. Left, Left hemisphere; Right, right hemisphere.

handers, making comparison between the groups difficult, based on the previous evidence, we conclude that the inclusion of left- and mixed-handed participants benefitted rather than limited the study.

We next asked whether structural variability within the frontoparietal networks mediates differences in visual attention abilities by correlating TVA-based parameters and tractography derived indices of microstructural variability (the HMOA) and macrostructural variability (tract volume). Our data, as presented below, indicate that the microstructural and macrostructural organization of the frontoparietal pathways differentially contributes to individual differences in attentional functions.

When we examined microstructural measures, we found that individual differences in K (VSTM capacity) were linked to variability in the SLF II and SLF III as well as the IFOF within the right hemisphere (Fig. 6*A*). Specifically, higher VSTM capacity corresponded to a higher HMOA within the right SLF II ($r = 0.54$, $p = 0.005$, FDR corrected), the right SLF III ($r = 0.43$, $p = 0.022$, FDR corrected), and the right IFOF ($r = 0.47$, $p = 0.018$, FDR corrected). By contrast, the HMOA index within the three branches of the SLF within the left hemisphere and the left IFOF was not correlated with VSTM capacity (FDR corrected p values not significant, i.e., $p > 0.1$). VSTM capacity was also correlated with the LI of SLF II and IFOF (SLF II, $r = 0.44$, $p = 0.021$, FDR corrected; IFOF, $r = 0.46$, $p = 0.018$, FDR corrected; Fig. 6*A*). Similarly to VSTM capacity, the higher speed of visual information processing based on TVA-derived parameter C was associated with a higher HMOA within the right SLF II and the right SLF III, although these correlations were not as strong as in case of VSTM capacity and have not survived corrections for multiple comparisons ($r = 0.29$, $p = 0.046$ uncorrected/$p = 0.22$ FDR corrected and $r = 0.29$, $p = 0.047$ uncorrected/$p = 0.22$ FDR corrected). The speed of visual information processing was also positively correlated with hemispheric lateralization of the IFOF ($r = 0.38$, $p < 0.051$, FDR corrected; Fig. 6*B*). All other correlations between microstructural properties of frontoparietal pathways and parameter C were not significant (p values not significant, i.e., $p > 0.1$).

In addition to the K and C parameters, TVA also assesses attentional spatial bias quantified by ω_{index} (i.e., the laterality index of the relative balance between attentional weights in the left versus right visual fields). Our analysis found ω_{index} to be negatively correlated with HMOA measure within the right SLF II ($r = -0.43$, $p < 0.022$ FDR corrected; Fig. 6*C*), thus indicating that lower HMOA within the right SLF II corresponded to the larger attentional weights assigned to elements in the left visual hemifield. All other correlations between microstructural properties of frontoparietal pathways and ω_{index} were not significant (p values not significant, i.e., $p > 0.1$).

Finally, none of the correlations between the microstructural properties (HMOA index) of all four examined frontoparietal pathways within the left and right hemispheres and the t_0 parameter (i.e., the minimum exposure duration for conscious visual detection) and the α parameter (i.e., top-down controlled selection) was statistically significant ($p > 0.1$).

When we assessed correlations between TVA parameters and the macrostructural measures (fiber tract volume), we found that the volume of the SLF II within the right hemisphere was positively correlated with the ω_{index} ($r = 0.34$, $p = 0.021$ FDR corrected), indicating that a larger volume of the right SLF II corresponded to a greater leftward bias. There were no other statistically significant ($p > 0.1$) correlations between the volume of any of the examined WM pathways within both hemispheres and the TVA-derived parameters.

Similarly to the assessment of lateralization of frontoparietal pathways, we also repeated correlation analyses between TVA-based parameters and microstructural and macrostructural variability measures, while excluding left-handed and ambidextrous participants. Again, we found results very similar to those based on the entire group of participants (Table 3).

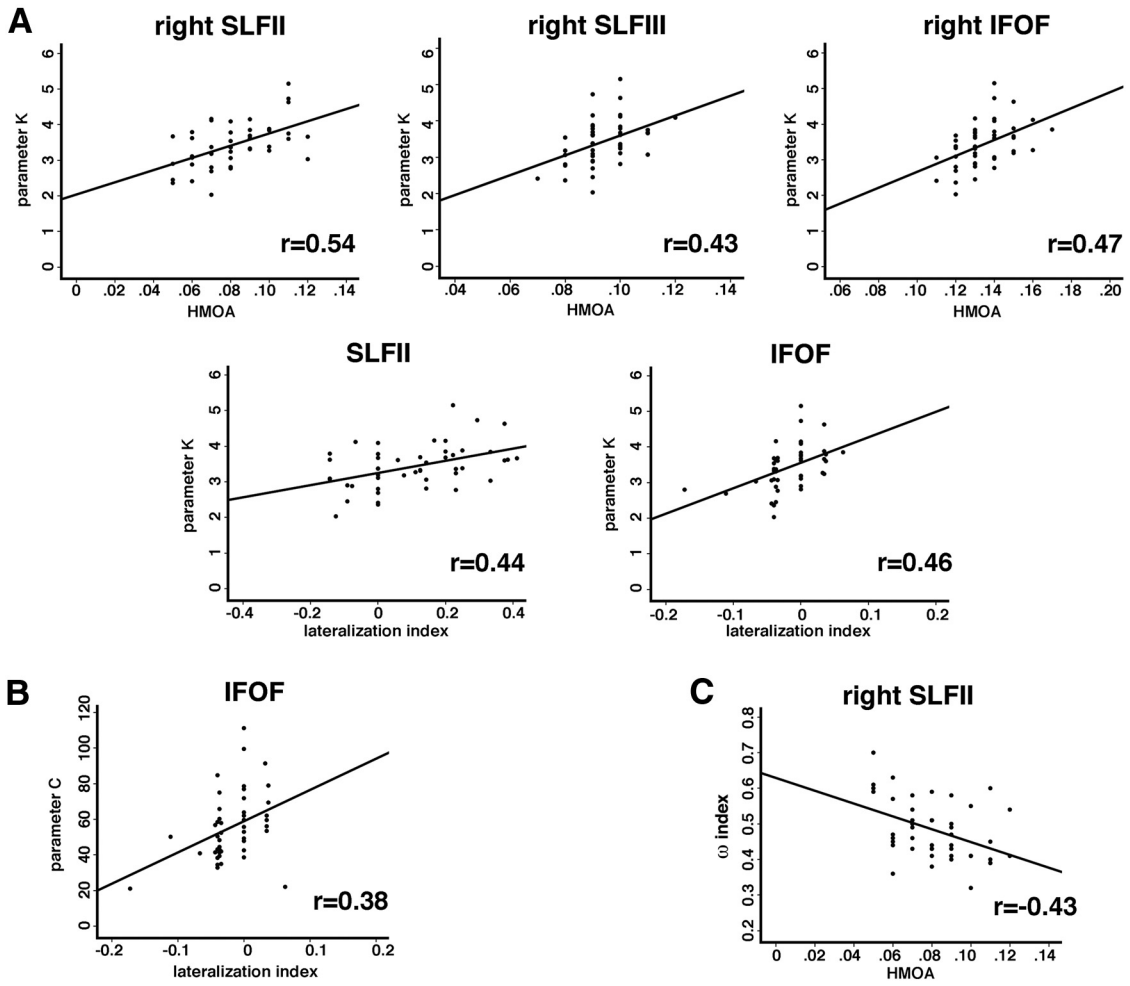

Figure 6. Relationship between structural variability and individual differences in attentional abilities. ***A***, Correlations between visual short-term memory capacity (parameter K) and HMOA measures within the right frontoparietal pathways (SLF II and SLF III and IFOF) and the HMOA-derived SLF II and IFOF lateralization indices. ***B***, Correlations between speed of information processing (parameter C) and the HMOA-derived IFOF LI. ***C***, Correlations between attentional spatial bias (ω_{index}) and HMOA measures within the right SLF II.

Finally, subsequent correlation analyses between the raw data (Fig. 2) and microstructural and macrostructural measures of structural variability within the frontoparietal networks showed very similar results (Table 4) to the ones reported above indicating that our findings can be generalized. In the paper, we favor a TVA-based analysis as the TVA model estimates are not only reliable and stable (Habekost et al., 2014) but may also directly interpreted within a reputed cognitive theory.

Discussion

One of the critical questions for cognitive neuroscience is how variability in the structural and functional organization of the human brain affects cognitive performance. Here we examined whether structural variability within frontoparietal WM pathways mediates individual differences in visual attention measured using Bundesen's TVA (Bundesen, 1990). Our data indicate that the HMOA, indexing the microstructural organization, and tract volume, indexing macrostructural organization of WM pathways, differentially contribute not only to the anatomical lateralization of frontoparietal attentional networks but also to individual differences in attention. Furthermore, we show that individual differences in attentional functions, such as in VSTM capacity, processing speed, and spatial bias, as assessed by the TVA framework, link to variability in structural organization within frontoparietal pathways (for evidence on the effects of aging, see also Espeseth et al., 2014).

Lateralization of frontoparietal networks

In the normal population, there is a reliable leftward attentional bias when performing many cognitive tasks, commonly attributed to right hemispheric dominance in spatial attention (Kinsbourne, 1977; Mesulam, 1981). It has been suggested that the preferential activation of the right hemisphere leads to leftward attentional bias, but the functional lateralization is by no means universal and does not apply to the entire frontoparietal attentional networks (Doricchi et al., 2010; Shulman et al., 2010). Interestingly, functional neuroimaging studies not only point to hemispheric asymmetries in the representation of visual space in VSTM and spatial attention, especially within the posterior parietal cortex, but also indicate task-dependent and topographic region-dependent properties of these asymmetries. For example, it has been shown that some of the topographic areas within posterior parietal cortex have a weaker contralateral bias in the right hemisphere compared with the left (Sheremata et al., 2010; Szczepanski and Kastner, 2013; Sheremata and Silver, 2015).

The anatomical foundations of the right hemisphere dominance of attention are not fully understood. To date, only one study has specifically investigated the structural basis of this dom-

Table 3. Results of the correlation analyses between the TVA-based parameters and microstructural and macrostructural measures of structural variability within the frontoparietal networks in the group of only right-handed participants ($n = 31$)[a]

TVA parameters	Significant correlations
Parameter K (VSTM capacity)	$r = 0.60; p = 0.005$, FDR corrected (HMOA right SLF II)
	$r = 0.51; p = 0.017$, FDR corrected (HMOA right SLF III)
	$r = 0.47; p = 0.025$, FDR corrected (HMOA right IFOF)
	$r = 0.48; p = 0.025$, FDR corrected (HMOA lateralization SLF II)
	$r = 0.52; p = 0.017$, FDR corrected (HMOA lateralization IFOF)
Parameter C (speed of information processing)	$r = 0.43; p = 0.025$, FDR corrected (HMOA lateralization IFOF)
ω_{index} (spatial bias)	$r = -0.42; p = 0.043$, FDR corrected (HMOA right SLF II)
	$r = 0.41; p = 0.046$, FDR corrected (volume right SLF II)

[a]All other correlations between microstructural and macrostructural properties of frontoparietal pathways and TVA-based parameters were not significant (p values not significant i.e. $p > 0.1$).

Table 4. Results of the correlation analyses between the raw data (Figure 2) and microstructural and macrostructural measures of structural variability within the frontoparietal networks

Raw data measure	Significant correlations
Whole report: 6 letter condition (no. of reported letters)[a]	$r = 0.48; p = 0.003$, FDR corrected (HMOA right SLF II)
	$r = 0.43; p = 0.006$, FDR corrected (HMOA right SLF III)
	$r = 0.30; p = 0.05$, FDR corrected (HMOA right IFOF)
	$r = 0.40; p = 0.01$, FDR corrected (HMOA lateralization SLF II)
	$r = 0.35; p = 0.02$, FDR corrected (HMOA lateralization IFOF)
Difference between the no. of correctly reported letters at 10 and 80 ms[b]	$r = 0.47; p = 0.003$, FDR corrected (HMOA lateralization SLF II)
	$r = 0.42; p = 0.005$, FDR corrected (HMOA lateralization IFOF)
Spatial bias[c]	$r = 0.32; p = 0.03$, FDR corrected (volume right SLF II)
	$r = -0.38; p = 0.01$, FDR corrected (HMOA right SLF II)

[a]The raw scores for the whole report: 6 target letter condition (measuring the no. of reported letters at the longest exposure duration, i.e., 200 ms) corresponding to TVA parameter K.

[b]The difference in the raw scores between the no. of correctly reported letters at 10 and 80 ms corresponding to TVA parameter C.

[c]Spatial bias based on the raw data = lateralization index left/(left + right) calculated based on the raw scores for the left and right visual fields, corresponding to the TVA-based laterality index (ω_{index}).

Only significant correlations are reported.

inance, focusing on lateralization of the superior longitudinal fasciculus based on tract volume measures and showing that only the ventral branch, SLF III, is right lateralized (Thiebaut de Schotten et al., 2011). Here we extended these findings by examining structural lateralization within frontoparietal pathways (SLF and IFOF) based on not only volume but also on the HMOA index. Whereas tract volume reflects the macrostructural characteristics of WM pathways, HMOA is influenced by microstructural properties, including myelination, axon density, axon diameter, and fiber dispersion (Dell'Acqua et al., 2013). In agreement with previous reports (Thiebaut de Schotten et al., 2011), we too found that the ventral branch of the SLF, SLF III, was right lateralized based on measures of tract volume. However, based on the HMOA index, we found a different pattern of lateralization within frontoparietal pathways, with SLF II and IFOF being right lateralized. This discrepancy between lateralization indices within the frontoparietal pathways based on microstructural and macrostructural measures is not entirely surprising taking into account that HMOA and tract volume reflect very different properties of WM pathways. Whereas HMOA represents a surrogate of tissue density (tissue microstructure) (Dell'Acqua et al., 2013), the track volume, which is calculated as the number of voxels intersected by the reconstructed streamlines, denotes the space occupied by the tract (macrostructure) and its relationship to axonal number, axonal diameter, and density has yet to be established (Beaulieu, 2002). The findings that HMOA and tract volume differentially contribute to the anatomical lateralization of frontoparietal attentional networks are in agreement with previous studies showing that the asymmetry of WM pathways varies across different measures derived from diffusion MRI (De Santis et al., 2014). A remaining question, which cannot be answered by the current study, is whether variability in WM organization and in structural lateralization is reflected in individual differences in functional connectivity and/or preferential right hemisphere activation during visuospatial attention tasks.

The macrostructural lateralization within SLF III, interconnecting the ventral network, fits well with functional neuroimaging studies reporting asymmetrical activation of cortical loci within the right ventral attention network during tasks requiring stimulus-driven shifts of attention and target detection (Corbetta and Shulman, 2002; Shulman et al., 2010). But while right hemisphere dominance has been reported only within the ventral network, by contrast, it has been shown consistently that the dorsal not ventral network controls the allocation of attention to a particular location in space. To account for these "functional discrepancies" between dorsal and ventral regions, Corbetta and Shulman (2011) suggested that spatial biases in visual attention result from direct interactions between dorsal and ventral regions. Thus, our findings indicating right microstructural lateralization of SLF II, which interconnects the dorsal and ventral networks (Makris et al., 2005; Schmahmann and Pandya, 2006; Thiebaut de Schotten et al., 2011), are in line with this proposal.

Thiebaut de Schotten et al. (2011) also reported individual variability in the structural organization of attention networks, showing, for example, striking variation in SLF II lateralization with some individuals having larger volume of SLF II within the right hemisphere and some within the left hemisphere. Similarly, we found striking individual variability in lateralization within frontoparietal pathways (Fig. 6), with some individuals having larger volume and/or HMOA index within the right and some within the left hemisphere.

Structural variability mediates individual differences in attention

Thiebaut de Schotten et al. (2011) provided a first demonstration that variation in tract volume within SLF II predicts spatial biases. Here we substantially extended these earlier findings by combining the evaluation of microstructure and macrostructure indices of frontoparietal attention pathways with quantitative analysis of the different facets of attention according to the TVA framework (Bundesen, 1990). TVA assumes that visual processing starts with parallel matching of stimuli to representations in visual long-term memory. This first matching stage is followed by a race (competition) between representations of the elements

for entry into VSTM. The efficiency of the match and race processes can be characterized through parameters reflecting attentional weighting between the left and right visual field (spatial bias), the minimum effective exposure duration, the top-down controlled selection, the speed of processing, and VSTM capacity (Bundesen, 1998).

In agreement with Thiebaut de Schotten et al. (2011), we found that lateralization of SLF II volume correlated with spatial bias: a larger SLF II volume within the right hemisphere corresponded to a larger assignment of attentional weight to elements in the left visual hemifield. Strikingly, we found no other correlations between the volume of frontoparietal pathways and any measure of TVA-derived attentional abilities. In contrast, we demonstrated strong links between microstructural properties of frontoparietal pathways and individual differences in attentional functions, VSTM capacity, processing speed, and spatial bias. Specifically, a higher HMOA within the right SLF II, SLF III, and IFOF was associated with higher VSTM capacity. Although functional neuroimaging studies (e.g., Gillebert et al., 2012) found that activity within intraparietal sulcus (dorsal network) correlated with VSTM capacity, these findings show that communication between the dorsal and ventral networks via interconnecting tracts might be a contributing factor. We also found positive correlations between VSTM capacity and the LI of SLF II and the IFOF, as well as between lateralization of the IFOF and speed of information processing. However, spatial biases in attention were negatively correlated with the HMOA within the right SLF II, indicating that lower HMOA within the right SLF II corresponded to the larger attentional weights assigned to elements in the left visual hemifield. Although these opposite correlations found for VSTM capacity and spatial bias seem somewhat surprising, our behavioral data indicated a weak negative correlation between K and ω_{index}. It is also imperative to note that HMOA is estimated based on several WM characteristics, including myelination, axon density, axon diameter, and fiber dispersion (Dell'Acqua et al., 2013) and within each voxel these factors may differentially contribute to HMOA. Currently, it is not possible to separate these properties and hence to interpret differences in HMOA in linear fashion, for example, that higher HMOA is equivalent to higher connectivity (Beaulieu, 2002; Jones et al., 2013; Dell'Acqua et al., 2013). Nevertheless, as HMOA is specific to the direction followed by tractography, this index measures how much water is diffusing in the tractography reconstruction direction independently of other directions. Subsequently, it has been shown that HMOA decreases with increasing radial diffusivity and the axonal radius; thus, it is likely that increased myelination decreases HMOA (Tournier et al., 2004; Dell'Acqua et al., 2013). Moreover, we would like to point out that other investigators have previously reported different directions of correlations (positive vs negative) between microstructural properties of WM pathways and individual differences in cognitive abilities (Tuch et al., 2005; Roberts et al., 2010). Therefore, while we can argue that individual differences in attentional functions link to variability in structural organization within frontoparietal pathways, we should be cautious in inferring about directional changes in connectivity and microstructural properties contributing to the observed cognitive disparities. Nevertheless, we note that the links between right hemisphere lateralization in processing speed and VSTM capacity fit with arguments that these nonspatial factors can be selectively disrupted by right hemisphere damage in patients with neglect (Malhotra et al., 2005) and simultanagnosia (Chechlacz et al., 2012). The present results point to the neural lateralization of nonspatial as well as spatial aspects of visual attention. Furthermore, our findings indicating a strong association between individual differences in VSTM capacity and structural (anatomical) lateralization within frontoparietal networks agree with extensive evidence that functional hemispheric asymmetries within posterior parietal cortex are linked to laterality bias in VSTM (Sheremata et al., 2010; Somers and Sheremata, 2013; Sheremata and Silver, 2015).

In conclusion, individual differences in the weighting of spatial attention in the left and right visual fields are associated with variability within the right SLF II interconnecting the dorsal and ventral networks are consistent with the proposal by Corbetta and Shulman (2011) that spatial biases result from direct interactions between dorsal and ventral regions. These findings are also in agreement with direct evidence linking pathological rightward bias in neglect patients with damage to the right SLF II (Thiebaut de Schotten et al., 2014). In contrast to spatial bias, we show that differences in VSTM capacity are linked to structural variability within SLF III, interconnecting cortical loci within the ventral attentional network and both VSTM capacity and speed of information processing (both "nonspatial" aspects of visual attention) are linked to variability in hemispheric lateralization within IFOF and SLF II, two pathways interconnecting the dorsal and ventral networks (Petrides and Pandya, 1984, 1988, 2002; Makris et al., 2005; Petrides and Pandya, 2006; Schmahmann and Pandya, 2006; Thiebaut de Schotten et al., 2011). These later findings support a notion of interactive neural substrates supporting the integration of spatial and nonspatial cognitive mechanisms of attention. Specifically, we propose that spatial asymmetries (spatial biases) are modulated by nonspatial facets of attention as a result of network interactions within the right hemisphere. Thus, microstructural lateralization within IFOF and SLF II, two pathways interconnecting the dorsal and ventral networks, might provide the basis for right hemisphere advantages in terms of attentional capacity and speed of information processing.

It is plausible that the lack of correlations between structural variability within frontoparietal pathways and other visual attention parameters derived from TVA (the minimum exposure duration for conscious visual perception and the top-down controlled selection) is due to the fact that our analysis lacked power because of insufficient overall behavioral variability in the participants or the task not being sensitive enough to detect sufficient behavioral variability. This awaits further research. Also, in the current study, we have not excluded participants based on handedness, and we had a large number of right-handers compared with left- and mixed-handers as expected based on typical population distribution (Willems et al., 2014). Such inclusion criteria not only limit any direct comparisons between participants with different handedness but also mean that interpretation of lateralization results, especially generalization to different populations, should be made with caution.

References

Andersson JL, Skare S, Ashburner J (2003) How to correct susceptibility distortions in spin-echo echo-planar images: application to diffusion tensor imaging. Neuroimage 20:870–888. CrossRef Medline

Badzakova-Trajkov G, Häberling IS, Roberts RP, Corballis MC (2010) Cerebral asymmetries: complementary and independent processes. PLoS One 5:e9682. CrossRef Medline

Bartolomeo P, Thiebaut de Schotten M, Doricchi F (2007) Left unilateral neglect as a disconnection syndrome. Cereb Cortex 17:2479–2490. CrossRef Medline

Beaulieu C (2002) The basis of anisotropic water diffusion in the nervous system: a technical review. NMR Biomed 15:435–455. CrossRef Medline

Benjamini Y, Hochberg Y (1995) Controlling the false discovery rate: a practical and powerful approach to multiple testing. J R Stat Soc B 57:289–300.

Boorman ED, O'Shea J, Sebastian C, Rushworth MF, Johansen-Berg H (2007) Individual differences in white-matter microstructure reflect variation in functional connectivity during choice. Curr Biol 17:1426–1431. CrossRef Medline

Bryden MP, Hécaen H, DeAgostini M (1983) Patterns of cerebral organization. Brain Lang 20:249–262. CrossRef Medline

Bundesen C (1990) A theory of visual attention. Psychol Rev 97:523–547. CrossRef Medline

Bundesen C (1998) A computational theory of visual attention. Philos Trans R Soc Lond B Biol Sci 353:1271–1281. CrossRef Medline

Bundesen C, Habekost T, Kyllingsbaek S (2005) A neural theory of visual attention: bridging cognition and neurophysiology. Psychol Rev 112:291–328. CrossRef Medline

Cai Q, Van der Haegen L, Brysbaert M (2013) Complementary hemispheric specialization for language production and visuospatial attention. Proc Natl Acad Sci U S A 110:E322-E330. CrossRef Medline

Catani M, Thiebaut de Schotten M (2008) A diffusion tensor imaging tractography atlas for virtual in vivo dissections. Cortex 44:1105–1132. CrossRef Medline

Chang H, Fitzpatrick JM (1992) A technique for accurate magnetic resonance imaging in the presence of field inhomogeneities. IEEE Trans Med Imaging 11:319–329. CrossRef Medline

Chechlacz M, Rotshtein P, Hansen PC, Riddoch JM, Deb S, Humphreys GW (2012) The neural underpinings of simultanagnosia: disconnecting the visuospatial attention network. J Cogn Neurosci 24:718–735. CrossRef Medline

Corbetta M, Shulman GL (2002) Control of goal-directed and stimulus-driven attention in the brain. Nat Rev Neurosci 3:201–215. CrossRef Medline

Corbetta M, Shulman GL (2011) Spatial neglect and attention networks. Annu Rev Neurosci 34:569–599. CrossRef Medline

Dell'Acqua F, Scifo P, Rizzo G, Catani M, Simmons A, Scotti G, Fazio F (2010) A modified damped Richardson-Lucy algorithm to reduce isotropic background effects in spherical deconvolution. Neuroimage 49:1446–1458. CrossRef Medline

Dell'Acqua F, Simmons A, Williams SC, Catani M (2013) Can spherical deconvolution provide more information than fiber orientations? Hindrance modulated orientational anisotropy, a true-tract specific index to characterize white matter diffusion. Hum Brain Mapp 34:2464–2483. CrossRef Medline

De Santis S, Drakesmith M, Bells S, Assaf Y, Jones DK (2014) Why diffusion tensor MRI does well only some of the time: variance and covariance of white matter tissue microstructure attributes in the living human brain. Neuroimage 89:35–44. CrossRef Medline

Desimone R, Duncan J (1995) Neural mechanisms of selective visual attention. Annu Rev Neurosci 18:193–222. CrossRef Medline

Doricchi F, Thiebaut de Schotten M, Tomaiuolo F, Bartolomeo P (2008) White matter (dis)connections and gray matter (dys)functions in visual neglect: gaining insights into the brain networks of spatial awareness. Cortex 44:983–995. CrossRef Medline

Doricchi F, Macci E, Silvetti M, Macaluso E (2010) Neural correlates of the spatial and expectancy components of endogenous and stimulus-driven orienting of attention in the Posner task. Cereb Cortex 20:1574–1585. CrossRef Medline

Duncan J, Humphreys G, Ward R (1997) Competitive brain activity in visual attention. Curr Opin Neurobiol 7:255–261. CrossRef Medline

Dyrholm M, Kyllingsbaek S, Espeseth T, Bundesen C (2011) Generalizing parametric models by introducing trial-by-trial parameter variability: the case of TVA. J Math Psychol 55:416–429. CrossRef

Espeseth T, Vangkilde SA, Petersen A, Dyrholm M, Westlye LT (2014) TVA-based assessment of attentional capacities-associations with age and indices of brain white matter microstructure. Front Psychol 5:1177. CrossRef Medline

Finke K, Bublak P, Krummenacher J, Kyllingsbaek S, Muller HJ, Schneider WX (2005) Usability of a theory of visual attention (TVA) for parameter-based measurement of attention: I. Evidence from normal subjects. J Int Neuropsychol Soc 11:832–842. Medline

Flöel A, Buyx A, Breitenstein C, Lohmann H, Knecht S (2005) Hemispheric lateralization of spatial attention in right- and left-hemispheric language dominance. Behav Brain Res 158:269–275. CrossRef Medline

Frost MA, Goebel R (2012) Measuring structural-functional correspondence: spatial variability of specialised brain regions after macro-anatomical alignment. Neuroimage 59:1369–1381. CrossRef Medline

Gillebert CR, Dyrholm M, Vangkilde S, Kyllingsbaek S, Peeters R, Vandenberghe R (2012) Attentional priorities and access to short-term memory: parietal interactions. Neuroimage 62:1551–1562. CrossRef Medline

Habekost T, Bundesen C (2003) Patient assessment based on a theory of visual attention (TVA): subtle deficits after a right frontal-subcortical lesion. Neuropsychologia 41:1171–1188. CrossRef Medline

Habekost T, Rostrup E (2006) Persisting asymmetries of vision after right side lesions. Neuropsychologia 44:876–895. CrossRef Medline

Habekost T, Petersen A, Vangkilde S (2014) Testing attention: comparing the ANT with TVA-based assessment. Behav Res Methods 46:81–94. CrossRef Medline

Jones DK, Knösche TR, Turner R (2013) White matter integrity, fiber count, and other fallacies: the do's and don'ts of diffusion MRI. Neuroimage 73:239–254. CrossRef Medline

Kinsbourne M (1977) Hemi-neglect and hemisphere rivalry. Adv Neurol 18:41–49. Medline

Kyllingsbaek S (2006) Modeling visual attention. Behav Res Methods 38:123–133. CrossRef Medline

Makris N, Kennedy DN, McInerney S, Sorensen AG, Wang R, Caviness VS Jr, Pandya DN (2005) Segmentation of subcomponents within the superior longitudinal fascicle in humans: a quantitative, in vivo, DT-MRI study. Cereb Cortex 15:854–869. CrossRef Medline

Malhotra P, Jäger HR, Parton A, Greenwood R, Playford ED, Brown MM, Driver J, Husain M (2005) Spatial working memory capacity in unilateral neglect. Brain 128:424–435. CrossRef Medline

Mazoyer B, Zago L, Jobard G, Crivello F, Joliot M, Perchey G, Mellet E, Petit L, Tzourio-Mazoyer N (2014) Gaussian mixture modeling of hemispheric lateralization for language in a large sample of healthy individuals balanced for handedness. PLoS One 9:e101165. CrossRef Medline

Mesulam MM (1981) A cortical network for directed attention and unilateral neglect. Ann Neurol 10:309–325. CrossRef Medline

Mesulam MM (1990) Large-scale neurocognitive networks and distributed processing for attention, language, and memory. Ann Neurol 28:597–613. CrossRef Medline

Mori S, Kaufmann WE, Davatzikos C, Stieltjes B, Amodei L, Fredericksen K, Pearlson GD, Melhem ER, Solaiyappan M, Raymond GV, Moser HW, van Zijl PC (2002) Imaging cortical association tracts in the human brain using diffusion-tensor-based axonal tracking. Magn Reson Med 47:215–223. CrossRef Medline

Mueller S, Wang D, Fox MD, Yeo BT, Sepulcre J, Sabuncu MR, Shafee R, Lu J, Liu H (2013) Individual variability in functional connectivity architecture of the human brain. Neuron 77:586–595. CrossRef Medline

Neisser U (1967) Cognitive psychology. Englewood Cliffs, NJ: Prentice-Hall.

Oldfield RC (1971) The assessment and analysis of handedness: the Edinburgh Inventory. Neuropsychologia 9:97–113. CrossRef Medline

Petit L, Zago L, Mellet E, Jobard G, Crivello F, Joliot M, Mazoyer B, Tzourio-Mazoyer N (2015) Strong rightward lateralization of the dorsal attentional network in left-handers with right sighting-eye: an evolutionary advantage. Hum Brain Mapp 36:1151–1164. CrossRef Medline

Petrides M, Pandya DN (1984) Projections to the frontal cortex from the posterior parietal region in the rhesus monkey. J Comp Neurol 228:105–116. CrossRef Medline

Petrides M, Pandya DN (1988) Association fiber pathways to the frontal cortex from the superior temporal region in the rhesus monkey. J Comp Neurol 273:52–66. CrossRef Medline

Petrides M, Pandya DN (2002) Comparative cytoarchitectonic analysis of the human and the macaque ventrolateral prefrontal cortex and corticocortical connection patterns in the monkey. Eur J Neurosci 16:291–310. CrossRef Medline

Petrides M, Pandya DN (2006) Efferent association pathways originating in the caudal prefrontal cortex in the macaque monkey. J Comp Neurol 498:227–251. CrossRef Medline

Rademacher J, Bürgel U, Geyer S, Schormann T, Schleicher A, Freund HJ, Zilles K (2001) Variability and asymmetry in the human precentral motor system: a cytoarchitectonic and myeloarchitectonic brain mapping study. Brain 124:2232–2258. CrossRef Medline

Roberts RE, Anderson EJ, Husain M (2010) Expert cognitive control and

individual differences associated with frontal and parietal white matter microstructure. J Neurosci 30:17063–17067. CrossRef Medline

Schmahmann JD, Pandya DN (2006) Fiber pathways of the brain. Oxford: Oxford UP.

Schmahmann JD, Pandya DN, Wang R, Dai G, D'Arceuil HE, de Crespigny AJ, Wedeen VJ (2007) Association fibre pathways of the brain: parallel observations from diffusion spectrum imaging and autoradiography. Brain 130:630–653. CrossRef Medline

Sheremata SL, Silver MA (2015) Hemisphere-dependent attentional modulation of human parietal visual field representations. J Neurosci 35:508–517. CrossRef Medline

Sheremata SL, Bettencourt KC, Somers DC (2010) Hemispheric asymmetry in visuotopic posterior parietal cortex emerges with visual short-term memory load. J Neurosci 30:12581–12588. CrossRef Medline

Shulman GL, Pope DL, Astafiev SV, McAvoy MP, Snyder AZ, Corbetta M (2010) Right hemisphere dominance during spatial selective attention and target detection occurs outside the dorsal frontoparietal network. J Neurosci 30:3640–3651. CrossRef Medline

Smith SM, Jenkinson M, Woolrich MW, Beckmann CF, Behrens TE, Johansen-Berg H, Bannister PR, De Luca M, Drobnjak I, Flitney DE, Niazy RK, Saunders J, Vickers J, Zhang Y, De Stefano N, Brady JM, Matthews PM (2004) Advances in functional and structural MR image analysis and implementation as FSL. Neuroimage 23 [Suppl 1]:S208-S219.

Somers DC, Sheremata SL (2013) Attention maps in the brain. Wiley Interdiscip Rev Cogn Sci 4:327–340. CrossRef Medline

Sommer IE, Ramsey NF, Mandl RC, Kahn RS (2002) Language lateralization in monozygotic twin pairs concordant and discordant for handedness. Brain 125:2710–2718. CrossRef Medline

Sotiropoulos SN, Jbabdi S, Xu J, Andersson JL, Moeller S, Auerbach EJ, Glasser MF, Hernandez M, Sapiro G, Jenkinson M, Feinberg DA, Yacoub E, Lenglet C, Van Essen DC, Ugurbil K, Behrens TE (2013) Advances in diffusion MRI acquisition and processing in the Human Connectome Project. Neuroimage 80:125–143. CrossRef Medline

Sugiura M, Friston KJ, Willmes K, Shah NJ, Zilles K, Fink GR (2007) Analysis of intersubject variability in activation: an application to the incidental episodic retrieval during recognition test. Hum Brain Mapp 28:49–58. CrossRef Medline

Szaflarski JP, Binder JR, Possing ET, McKiernan KA, Ward BD, Hammeke TA (2002) Language lateralization in left-handed and ambidextrous people: fMRI data. Neurology 59:238–244. CrossRef Medline

Szczepanski SM, Kastner S (2013) Shifting attentional priorities: control of spatial attention through hemispheric competition. J Neurosci 33:5411–5421. CrossRef Medline

Szczepanski SM, Pinsk MA, Douglas MM, Kastner S, Saalmann YB (2013) Functional and structural architecture of the human dorsal frontoparietal attention network. Proc Natl Acad Sci U S A 110:15806–15811. CrossRef Medline

Thiebaut de Schotten M, Dell'Acqua F, Forkel SJ, Simmons A, Vergani F, Murphy DG, Catani M (2011) A lateralized brain network for visuospatial attention. Nat Neurosci 14:1245–1246. CrossRef Medline

Thiebaut de Schotten M, Tomaiuolo F, Aiello M, Merola S, Silvetti M, Lecce F, Bartolomeo P, Doricchi F (2014) Damage to white matter pathways in subacute and chronic spatial neglect: a group study and 2 single-case studies with complete virtual "in vivo" tractography dissection. Cereb Cortex 24:691–706. CrossRef Medline

Tournier JD, Calamante F, Gadian DG, Connelly A (2004) Direct estimation of the fiber orientation density function from diffusion-weighted MRI data using spherical deconvolution. Neuroimage 23:1176–1185. CrossRef Medline

Treisman AM, Gelade G (1980) A feature-integration theory of attention. Cogn Psychol 12:97–136. CrossRef Medline

Tuch DS, Salat DH, Wisco JJ, Zaleta AK, Hevelone ND, Rosas HD (2005) Choice reaction time performance correlates with diffusion anisotropy in white matter pathways supporting visuospatial attention. Proc Natl Acad Sci U S A 102:12212–12217. CrossRef Medline

Vangkilde S, Bundesen C, Coull JT (2011) Prompt but inefficient: nicotine differentially modulates discrete components of attention. Psychopharmacology (Berl) 218:667–680. CrossRef Medline

Whitehouse AJ, Bishop DV (2009) Hemispheric division of function is the result of independent probabilistic biases. Neuropsychologia 47:1938–1943. CrossRef Medline

Willems RM, Van der Haegen L, Fisher SE, Francks C (2014) On the other hand: including left-handers in congnitive neuroscience and neurogenetics. Nat Rev Neurosci 15:193–201. CrossRef Medline